Discovery and Labeling of High-Affinity 3,4-Diarylpyrazolines as Candidate Radioligands for In Vivo Imaging of Cannabinoid Subtype-1 (CB$_1$) Receptors

Sean R. Donohue,*,[†,‡] Victor W. Pike,[†] Sjoerd J. Finnema,[‡] Phong Truong,[‡] Jan Andersson,[‡] Balázs Gulyás,[‡] and Christer Halldin[‡]

Molecular Imaging Branch, National Institute of Mental Health, National Institutes of Health, Bethesda, Maryland 20892, Karolinska Institutet, Department of Clinical Neuroscience, Psychiatry Section, Karolinska Hospital, S-17176 Stockholm, Sweden

Imaging of cannabinoid subtype-1 (CB$_1$) receptors in vivo with positron emission tomography (PET) is likely to be important for understanding their role in neuropsychiatric disorders and for drug development. Radioligands for imaging with PET are required for this purpose. We synthesized new ligands from a 3,4-diarylpyrazoline platform of which (−)-**12a** ((−)-3-(4-chlorophenyl)-N'-[(4-cyanophenyl)sulfonyl]-4-phenyl-4,5-dihydro-1H-pyrazole-1-carboxamidine) was found to have high-affinity and selectivity for binding to CB$_1$ receptors. (−)-**12a** and its lower affinity enantiomer ((+)-**12a**) were labeled with carbon-11 ($t_{1/2}$ = 20.4 min) using [^{11}C]cyanide ion as labeling agent and evaluated as PET radioligands in cynomolgus monkeys. After injection of [^{11}C](−)-**12a**, there was high uptake and retention of radioactivity across brain according to the rank order of CB$_1$ receptor densities. The distomer, [^{11}C](+)-**12a**, failed to give a sustained CB$_1$ receptor-specific distribution. Polar radiometabolites of [^{11}C](−)-**12a** appeared moderately slowly in plasma. Radioligand [^{11}C](−)-**12a** is promising for the study of brain CB$_1$ receptors and merits further investigation in human subjects.

Introduction

The psychotropic, analgesic, and healing properties of *Cannabis sativa* (marijuana) have been known throughout documented history.[1] As for some other plant-derived medications (e.g., opium), there has been significant abuse of marijuana mainly because of an accompanying feeling of relaxation and psychological "high".[2,3] Nevertheless, legitimate medical use of marijuana may extend to the treatment of chemotherapy-induced emesis,[4,5] appetite stimulation in acquired immune deficiency syndrome (AIDS^a),[6,7] and movement disorders caused by multiple sclerosis.[8,9]

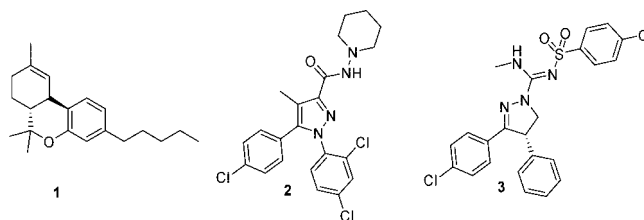* To whom correspondence should be addressed. Phone: 1-301-451-3909. Fax: 1-301-480-5112. E-mail: donohues@intra.nimh.gov. Address: Molecular Imaging Branch, National Institute of Mental Health, National Institutes of Health, Building 10, Rm B3 C342, 10 Center Drive, Bethesda, MD 20892-1003.

† Molecular Imaging Branch, National Institute of Mental Health, National Institutes of Health.

‡ Karolinska Institutet, Department of Clinical Neuroscience, Psychiatry Section, Karolinska Hospital.

^{a} Abbreviations: ACS, American Chemical Society; AIDS, acquired immune deficiency syndrome; BSA, bovine serum albumin; CB$_1$, cannabinoid subtype-1; CB$_2$, cannabinoid subtype-2; CRADA, Cooperative Research and Development Agreement; DAT, dopamine transporter; DMSO, dimethyl sulfoxide; DOR, δ opioid receptor; DTT, dithiothreitol; ee, enantiomeric excess; EDTA, ethylene diamine tetraacetic acid; fwhm, full-width at half-maximum; GTPγS, guanosine-5′-(γ-thio)-triphosphate; H, histamine receptor; HEPES, 4-(2-hydroxyethyl)-1-piperazineethanesulfonic acid; HPLC, high-performance liquid chromatography; HRMS, high-resolution mass spectrometry; K 2.2.2, 4,7,13,16,21,24-hexaoxa-1,10-diazabicyclo[8.8.8]hexacosane; KI, Karolinska Institutet; KOR, κ opioid receptor; LC-MS, liquid chromatography–mass spectrometry; MeCN, acetonitrile; MOR, μ opioid receptor; MRI, magnetic resonance imaging; mp, melting point; MTBE, *tert*-butyl methyl ether; NET, norepinephrine transporter; NIH, National Institutes of Health; NIMH, National Institute of Mental Health; NMR, nuclear magnetic resonance; PDSP, Psychoactive Drug Screening Program; PET, positron emission tomography; PipISB, *N*-(4-fluoro-benzyl)-4-(3-(piperidin-1-yl)-indole-1-sulfonyl)benzamide; P-gp, permeability-glycoprotein; ppm, parts per million; SERT, serotonin transporter; SPECT, single-photon emission computed tomography; SUV, standardized uptake value; TEA, triethylamine; Δ^9-THC, Δ^9-tetrahydrocannabinol, VOI, volume of interest.

Figure 1. Structures of CB$_1$ receptor ligands (**1**−**3**).

Efforts to elucidate the biological response to marijuana intake have identified (−)-(6aR,10aR)-6,6,9-trimethyl-3-pentyl-6a,7,8,10a-tetrahydro-6H-benzo[c]chromen-1-ol, **1** (Δ^9-THC, Figure 1),[10,11] as its most abundant active compound. **1** interacts with two main receptor types, namely cannabinoid subtype-1 (CB$_1$) and cannabinoid subtype-2 (CB$_2$) receptors.[12,13] Two spliced variants of the CB$_1$ receptor have also been identified, CB$_{1A}$ and CB$_{1B}$.[14,15] CB$_1$ receptors are located throughout the body and have high densities in regions of the brain, such as the hippocampus, striatum, and basal ganglia.[16,17] By contrast, CB$_2$ receptors are located mainly in peripheral tissues and are associated with the immune system.[13,18,19]

In 1994, Sanofi-Synthlabo introduced 5-(4-chlorophenyl)-1-(2,4-dichloro-phenyl)-4-methyl-N-(piperidin-1-yl)-1H-pyrazole-3-carboxamide, **2** (SR141716A, rimonabant, Figure 1), as a high-affinity inverse agonist at CB$_1$ receptors.[20] **2** has recently gained approval for use in the European Union as a treatment for morbid obesity. The therapeutic use of **2** may extend to addiction and neurodegenerative disorders. Consequently, there has been a considerable effort by pharmaceutical industry to develop novel CB$_1$ receptor inverse agonist platforms. Solvay AB succeeded with the development of (4S)-3-(4-chlorophenyl)-N-methyl-N'-[(4-chlorophenyl)sulfonyl]-4-phenyl-4,5-dihydro-1H-pyrazole-1-carboxamidine, **3** (SLV319, Figure 1).[21−23]

Brain CB$_1$ receptors may be involved in several neuropsychiatric disorders. Currently, there is a need for suitable ligands that are amenable to labeling with positron-emitters for nonin-

Figure 2. Structures of [^{11}C]**4−6**, [^{18}F]**6**, [^{18}F]**7**, and [^{11}C]**8**. Asterisks denote position of radiolabel.

Scheme 1. Synthesis of 3,4-Diarylpyrazoline Derivatives^a
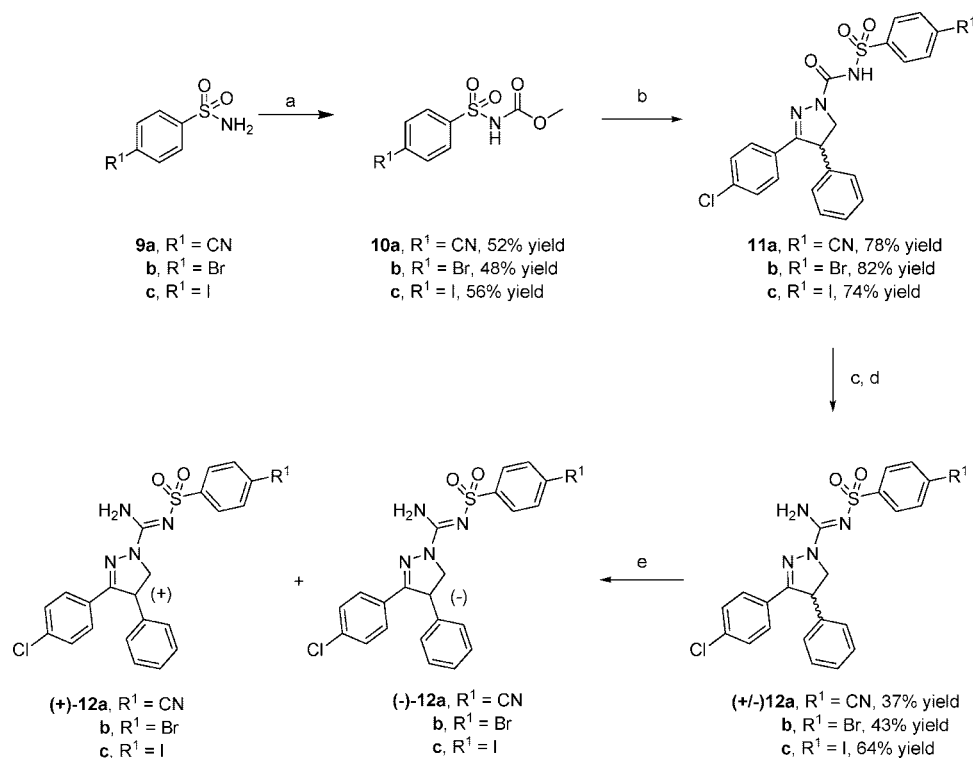
^{a} Conditions: (a) methyl chloroformate, TEA, MeCN; (b) 3-(4-chlorophenyl)-4,5-dihydro-4-phenyl-1*H*-pyrazole, toluene, reflux; (c) chlorobenzene, PCl$_5$; (d) methanolic NH$_3$; (e) ChiralPak AD, MeCN, 8 mL/min for **12a** and **12b** and 6 mL/min for **12c**.
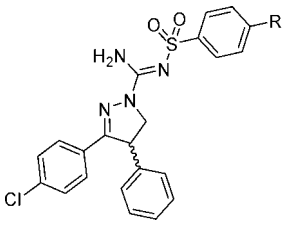
vasively imaging CB$_1$ receptors in vivo with PET under control and diseased states. Previous attempts at radioligand development have focused on the modification of the 1,5-diarylpyrazole CB$_1$ receptor class of **2** to allow for labeling with carbon-11 ($t_{1/2}$ = 20.4 min), fluorine-18 ($t_{1/2}$ = 109.7 min), or iodine-124 ($t_{1/2}$ = 4.15 d). Some success has been achieved with this approach (Figure 2), namely through the development of [^{11}C]**4** ([^{11}C]JHU75528)[24,25] and [^{11}C]**5** ([^{11}C]JHU75575).[25] Promising PET radioligands from other structural platforms have recently been reported (Figure 2) such as [^{11}C]**6** ([^{11}C]PipISB),[26] [^{18}F]**6** ([^{18}F]PipISB),[26] [^{18}F]**7** ([^{18}F]MK-9760),[27,28] and [^{11}C]**8** ([^{11}C]Me-PPEP).[29]

A 3,4-diarylpyrazoline class of CB$_1$ receptor ligand also presents favorable physiological and pharmacological attributes for PET radioligand development. The lead structure (**3**) shows high selectivity and potency for CB$_1$ receptors with little to no substrate behavior for P-glycoprotein (P-gp) efflux pumps.[22] Nevertheless, this structural class has remained largely unexplored for PET radioligand development. With this purpose in

mind, we have synthesized novel analogues of **3** that are amenable to radiolabeling. The CB$_1$ receptor affinities (K_i values) and selectivities were determined for the enantiomers of two ligands that were considered amenable to labeling with carbon-11 or radioiodine (e.g., iodine-123, $t_{1/2}$ = 13.13 h, or iodine-124). Additionally, one racemic ligand (**12a**), along with its eutomer and distomer, were labeled in high-specific radioactivity with [^{11}C]cyanide ion and investigated in monkeys with PET imaging. The emergence of radiometabolites in monkey plasma was measured with HPLC.

Results and Discussion

Chemistry. Ligands (**12a−c**) were synthesized by modifications of known general procedures (Scheme 1).[22] Briefly, the appropriate 4-substituted benzenesulfonamides (**9a−c**) were treated with methyl chloroformate plus triethylamine in acetonitrile to give the corresponding carbamic acid methyl esters (**10a−c**), which were then treated with 3-(4-chlorophenyl)-4,5-dihydro-4-phenyl-1*H*-pyrazole in toluene to give **11a−c** in good

Table 1. IC_{50} and K_i Values for the CB_1 and CB_2 Receptors and ClogP Data for Ligands **2**, (−)-**12a**, (+)-**12a**, (−)-**12c**, and (+)-**12c**

| ligand	R^1	CB_1 IC_{50} $(nM)^a$	CB_2 IC_{50} $(nM)^a$	CB_1 K_i $(nM)^a$	CB_2 K_i $(nM)^a$	$ClogP^b$
2		2.2 ± 0.5	4570 ± 410	0.4 ± 0.1	697 ± 63	6.95
(−)-**12a**	CN	2.8 ± 0.3	>33000	0.5 ± 0.1	>5000	3.85
(+)-**12a**	CN	100 ± 10	>33000	16.9 ± 2.0	>5000	3.85
(−)-**12c**	I	1.9 ± 0.7	>33000	0.3 ± 0.1	>5000	5.07
(+)-**12c**	I	103.5 ± 9.0	>33000	17.4 ± 2.0	>5000	5.07

^{a} Values are represent the mean ± SD of three determinations. ^{b} ClogP values were calculated by using the Pallas 3.0 software (Compudrug, USA).

yields. Treatment of **11a–c** with PCl_5 in chlorobenzene gave the crude imino chlorides, which were readily converted with methanolic NH_3 into the target ligands, **12a–c**. These ligands were then resolved into their enantiomers with chiral HPLC.

CB_1 and CB_2 in Vitro Binding Assays. High affinity is a prerequisite in candidate radioligands for PET imaging of neuroreceptors.[30] Generally, the more sparse the receptor the higher the affinity must be to permit successful imaging. As a guide, binding potentials represented by B_{max}/K_d should well exceed unity, when B_{max} and K_d (or as surrogate, K_i or IC_{50}) are expressed in nM.[30] CB_1 receptors are among the most abundant receptors in brain,[16,17] and hence moderately high affinity ($K_i < 10$ nM) may be acceptable. The IC_{50} and K_i values of rimonabant, (−)-**12a**, (+)-**12a**, (−)-**12c**, and (+)-**12c**, are shown in Table 1. The (−)-enantiomers exhibited high affinities for CB_1 receptors with IC_{50} values and K_is in low or sub nM range, respectively. These values compare well with other successful radioligands targeting CB_1 receptors, which generally have potencies or affinities in the nM range (e.g., [^{18}F]**7** and [^{11}C]**8**). The (+)-enantiomers of **12a** and **12c** exhibited lower CB_1 receptor affinities than their (−)-enantiomers; eudismic ratios were found to be about 35 for **12a** and 56 for **12c**. These ratios are similar to those of similar CB_1 receptor ligands from the 3,4-diarylpyrazoline class.[22] The eutomer of one such ligand has been shown to have the *S* configuration by X-ray crystallography.[22] Hence, the eutomers of **12a** and **12c** are also predicted to have *S* configuration.

Receptor Screening. Ligand (−)-**12a** showed <50% inhibition ($n = 4$) for the following receptors and binding sites: 5-HT_{1A-E}, 5-HT_{2B-C}, 5-HT_3, 5-HT_{5A}, 5-HT_6, 5-HT_7, $\alpha_{1A,B}$, α_{2A-C}, β_{1-3}, D_{1-5}, DAT, DOR, $H_{1,4}$, KOR, M_{1-5}, MOR, NET, SERT, $\sigma_{1,2}$. K_i values ($n = 3$) of $>7710 \pm 1110$ nM for the 5-HT_{2A} and >10000 nM for $H_{2,3}$ receptors were found. Hence, (−)-**12a** was found to have excellent CB_1 receptor selectivity for development as a PET radioligand.

Lipophilicities. The lipophilicity of a radioligand may critically influence its ability to penetrate the blood–brain barrier. Generally, a logP value in the range 2.0–3.5 is considered desirable for adequate brain entry without excessive nonspecific binding to brain tissue (i.e., fats, proteins).[31] ClogP is a useful tool for predicting lipophilicity trends among compounds of the same structural class.[30,31] ClogP was computed for (−)-**12a**, (+)-**12a**, (−)-**12c**, and (+)-**12c** (Table 1). Ligand **3** has previously been shown to penetrate the blood–brain

Scheme 2. Radiosynthesis of [^{11}C](±)-**12a** ^{a}
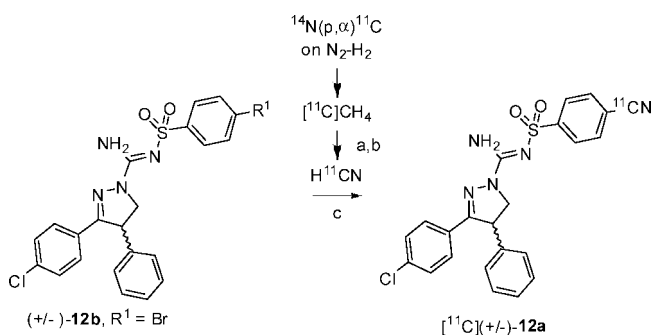
^{a} Conditions, reagents and decay-corrected yield: (a) Pt, NH_3 (20−30 mL/min), 990 °C; (b) 50% H_2SO_4, 90 °C; (c) $Pd(PPh_3)_4$, KOH, K2.2.2, DMSO, 110 °C, 36% ($n = 2$).

barrier despite its very high ClogP value (5.01).[22] The ClogP values of **12a** and its enantiomers are substantially lower (3.85) than that of **3** (Table 1), and hence they may be expected to enter brain readily. The values for **12c** and its enantiomers are similar to **3**, and hence they may also be expected to enter brain adequately.

Radiosynthesis. Initially, we set out to find an effective and rapid method for labeling **12** as its racemate. [^{11}C]Cyanide ion is a useful precursor for ^{11}C-labeling molecules with an aryl nitrile group.[32] The incorporation of [^{11}C]cyanide ion into an aryl ring is best achieved with copper[33,34] or palladium[32] catalyzed reactions. We considered each method for labeling (±)-**12a**. At first glance, [^{11}C]Cu(I)CN appears attractive for labeling PET radiopharmaceuticals. In general, use of this labeling agent requires one-pot and is insensitive to H_2O or NH_3 accompanying the production of [^{11}C]HCN. However, the overall radiochemical yields can be very low (e.g., 2.5%) and inferior to those from the palladium-catalyzed method.[34] Hence, the latter method was selected for labeling (±)-**12a**.

[^{11}C]HCN, which itself was prepared from cyclotron-produced [^{11}C]methane, was trapped in a DMSO solution of KOH and 4,7,13,16,21,24-hexaoxa-1,10-diazabicyclo[8.8.8]hexacosane (K 2.2.2), yielding a [^{11}C]CN^--K^+-K 2.2.2 complex, which was then added to the bromo precursor ((±)-**12b**) and $Pd(PPh_3)_4$ in DMSO and heated (Scheme 2). [^{11}C](±)-**12a** was separated from the crude product with reverse phase HPLC. The fraction containing [^{11}C](±)-**12a** was evaporated to dryness and formulated for safe intravenous injection. The overall radiosynthesis time was about 30 min. The nonoptimized decay-corrected yield was 36% ($n = 2$). There was no great improvement in yield when using the iodo compound (−)-**12c** as precursor. [^{11}C](±)-**12a** was obtained in high radiochemical purity (>98%) and was free of labeling precursors. Specific radioactivities were ≥56 GBq/µmol. Product identity was confirmed by liquid chromatography-mass spectrometry (LC-MS) of associated carrier and by coinjection with **12** in HPLC analysis and observation of coelution.

We attempted to prepare [^{11}C](−)-**12a** from precursor (−)-**12b** under the reaction conditions used to prepare [^{11}C](±)-**12a**. However, chiral HPLC analyses of the collected radioactive products revealed that complete racemization had occurred during the reactions (Table 2). Racemization was likely promoted by the strong base (KOH plus K 2.2.2) (Scheme 3).

To try to avoid racemization, several weaker bases were used in place of the KOH plus K 2.2.2. Interestingly, the use of $NaHCO_3$ as base gave [^{11}C](−)-**12a** to [^{11}C](+)-**12a** in a 9:1 ratio. Serendipitously, we found that the use of KH_2PO_4 (Table 2) gave [^{11}C](−)-**12a** in >94% ee ($n = 4$). These conditions were also used with (+)-**12c** as precursor, and the resulting

Table 2. Enantiomer Composition (%) of [¹¹C]**12a** after Treating (−)-**12b**, (−)-**12c**, or (+)-**12c** with [¹¹C]Cyanide Ion in DMSO in the Presence of Various Bases

precursor	base (a)	[¹¹C](−)-**12a** (%)	[¹¹C](+)-**12a** (%)
(−)-**12b**	KOH, K2.2.2	50	50
	NaHCO₃	90	10
(−)-**12c**	NaOAc	50	50
	NaHCO₃	90	10
	KH₂PO₄	>97 ($n = 4$)	<3 ($n = 4$)
(+)-**12c**	KH₂PO₄	<3 ($n = 1$)	>97 ($n = 1$)

product, [¹¹C](+)-**12a**, was obtained in >94% ee. The chemical identities of [¹¹C](−)-**12a** and [¹¹C](+)-**12a** were confirmed with LC-MS of associated carrier. Thus, [¹¹C](−)-**12a** and [¹¹C](+)-**12a** were obtained in high-chiral purity for evaluation as radioligands in monkeys with PET.

PET Measurements. After intravenous injection of [¹¹C](±)-**12a** into cynomolgus monkey, the brain radioactivity distributed according to the rank order of regional CB₁ receptor densities (Figure 3A). The highest radioactivity uptake was in CB₁ receptor-rich striatum, reaching 220% SUV at 30 min after injection. This slowly diminished to 180% SUV at 90 min after injection. The lowest maximal brain uptake was in pons reaching 150% SUV at 24 min after injection. The concentration of radioactivity in this region diminished to 124% SUV at 90 min after injection. In an experiment in which the CB₁ receptor-selective ligand **6** was given in high dose (1 mg/kg, iv) at 25 min after injection of [¹¹C](±)-**12a**, the regional brain radioactivity became homogeneous and diminished to about 95% SUV at 90 min after injection (Figure 3B). When **6** (1 mg/kg, iv) was given at 20 min before injection of [¹¹C](±)-**12a**, brain radioactivity became homogeneous and was characterized by a lower maximal uptake and fast washout, reaching 175% SUV at 15 min after injection and declining to 85% SUV at 90 min after injection (Figure 3C). These results demonstrated that a high proportion of brain radioactivity in the baseline experiment was reversibly bound to CB₁ receptors. The higher affinity enantiomer in this racemic radioligand was expected to be responsible for the majority of receptor-specific binding, while the lower affinity enantiomer was expected to bind mostly nonspecifically. We therefore set out to inject the homochiral radioligands, [¹¹C](−)-**12a** and [¹¹C](+)-**12a**, to test these expectations.

After intravenous injection of the higher affinity enantiomer, [¹¹C](−)-**12a**, into monkeys, the brain radioactivity again distributed according to the regional rank order of CB₁ receptor densities. The highest uptake of radioactivity was in striatum, reaching 200% SUV at 48 min after injection. The lowest maximal brain uptake was in the pons, reaching and maintaining ~125% SUV from 24 min after injection (Figure 4A). These time-activity curves are consistent with a high proportion of receptor-specific binding in all examined brain regions, as also seen in the experiment with racemic radioligand (Figure 3A).

In these experiments, as in PET imaging studies of other CB₁ receptor radioligands,[27,29] no region could be identified to represent nonspecific binding only. Pons does not serve this purpose because it contains some CB₁ receptors,[16,17,27] and measurements of its radioactivity concentration are contaminated from other nearby regions (e.g., CB₁ receptor-rich cerebellum) through the partial volume effect. In the absence of a reference region, ratios of specific to nonspecific binding cannot be estimated at all accurately by visual inspection of time-activity curves. Bolus plus constant infusion[35] or full kinetic compartmental model utilizing an arterial input function would be required to extract this information.[29]

By contrast with results from [¹¹C](−)-**12a**, after intravenous injection of the lower affinity enantiomer, [¹¹C](+)-**12a**, into monkeys, maximal brain radioactivity concentration reached 280% SUV at 1.5 min but then rapidly declined in all regions to about 95% SUV at 90 min (Figure 4B). These features of the time-activity curves are consistent with a high proportion of nonspecific binding in all examined regions and are consistent with the lower affinity of the radioligand.

Horizontal PET images obtained at the level of the striatum from data acquired between 9 and 93 min after injection of [¹¹C](−)-**12a** showed a distribution of radioactivity consistent with a large proportion of specific binding to CB₁ receptors, whereas corresponding images obtained with [¹¹C](+)-**12a** were strikingly homogeneous, indicating little receptor-specific binding (Figure 5).

Emergence of Radiometabolites of [¹¹C](−)-12a in Plasma. Analysis of venous samples showed that after injection of [¹¹C](−)-**12a** into cynomolgus monkeys, three less lipophilic radiometabolite fractions (t_Rs = 2.3, 5.8 and 8 min, cf. t_R = 8.5 min for [¹¹C](−)-**12a**) emerged in plasma (Figure 6A). Unchanged radioligand had declined to 50% of radioactivity in plasma at 45 min after injection (Figure 6B). The presence of the three radiometabolite fractions slowly increased as a percentage of total radioactivity in plasma throughout the scan. In this study, we did not determine the identities of any of these radiometabolite fractions nor whether they crossed the blood-brain barrier.

Finally, (−)-**12c** was not labeled with radioiodine in this study, but its properties (high affinity, high selectivity, and lipophilicity) suggest it has potential for development as a radioligand for imaging brain CB₁ receptors, either for PET or SPECT.

Conclusions

3,4-Diarylpyrazoline CB₁ ligands with high-affinity and selectivity for CB₁ receptors were discovered. One racemic ligand ((±)-**12a**), its eutomer ((−)-**12a**), and its distomer ((+)-**12a**) were successfully labeled with carbon-11 in high specific radioactivity. [¹¹C](−)-**12a** was found to be a promising radioligand for PET receptor imaging and merits further exploration in humans.

Experimental Section

Materials. All reagents were of ACS or HPLC quality and purchased from commercial sources and were used as received. 4-Cyanophenylsulfonamide, 4-bromophenylsulfonamide, and 4-iodophenylsulfonamide were synthesized by known procedures.[36] 3-(4-Chlorophenyl)-4,5-dihydro-4-phenyl-1*H*-pyrazole was also synthesized as reported.[37] **6** was provided by Eli Lilly and Co.

General Methods. ¹H (400 MHz) and ¹³C (100 MHz) NMR spectra were recorded at room temperature on an Avance-400 spectrometer (Brucker, Billerica, MA). Chemical shifts are reported in δ units (ppm) downfield relative to the chemical shift for tetramethylsilane. Signals are quoted as s (singlet), d (doublet), dd (double doublet), dt (double triplet), t (triplet), q (quartet), or m (multiplet). High-resolution mass spectra (HRMS) were determined using a time-of-flight electrospray instrument (University of Illinois at Urbana, Champaign, IL). Melting points (mp) were determined using a Mel-temp melting point apparatus (Electrothermal, Fisher Scientific, USA) and were uncorrected. Chiral HPLC, for the preparative resolution of racemates to enantiomers, was performed on a chiral column (ChiralPak AD, 20 mm × 250 mm) eluted with acetonitrile at 6 or 8 mL/min, as later specified. The enantiomeric excess (ee) of each resolved compound was measured by HPLC with the same method as used for resolution. Optical rotations ([α]$_D^{22}$) were measured with a P-1010 polarimeter (JASCO; Easton,
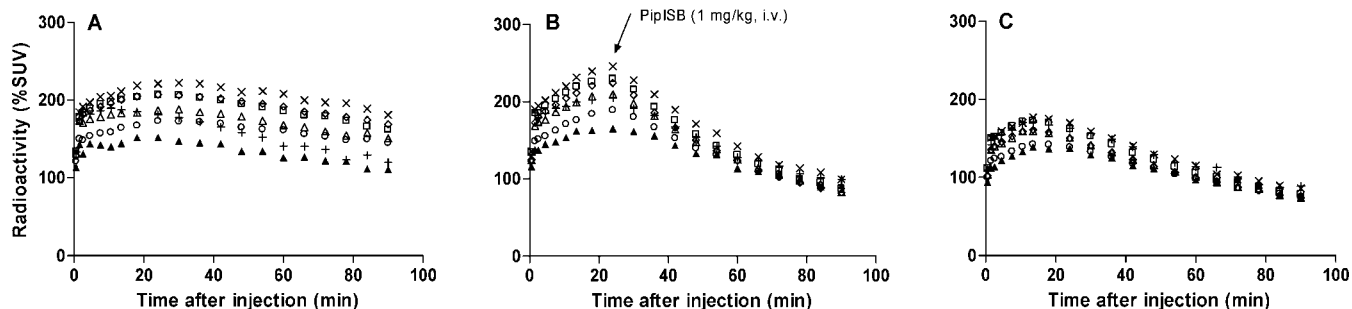
Figure 3. Regional time-radioactivity curves after iv injection of $[^{11}C](\pm)$-**12a** in cynomolgus monkey under baseline condition (A), with **6** (1 mg/kg, iv) administered as a displacing agent at 25 min (B), or pretreatment condition with **6** (1 mg/kg, iv) (C). Key: ×, striatum; △, cerebellum; ◇, frontal cortex; □, lateral temporal cortex; +, thalamus; ○, medial temporal cortex; ▲, pons.
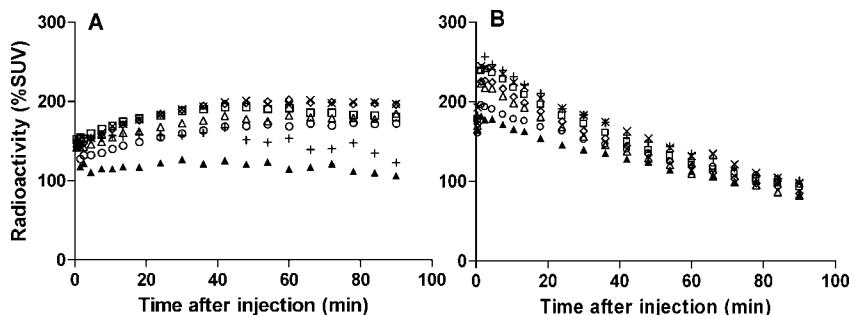

Figure 4. Regional time-radioactivity curves after iv injection of $[^{11}C](-)$-**12a** (100 MBq) (A) or $[^{11}C](+)$-**12a** (98 MBq) (B) in cynomolgus monkeys. Key: ×, striatum; △, cerebellum; ◇, frontal cortex; □, lateral temporal cortex; +, thalamus; ○, medial temporal cortex; ▲, pons.
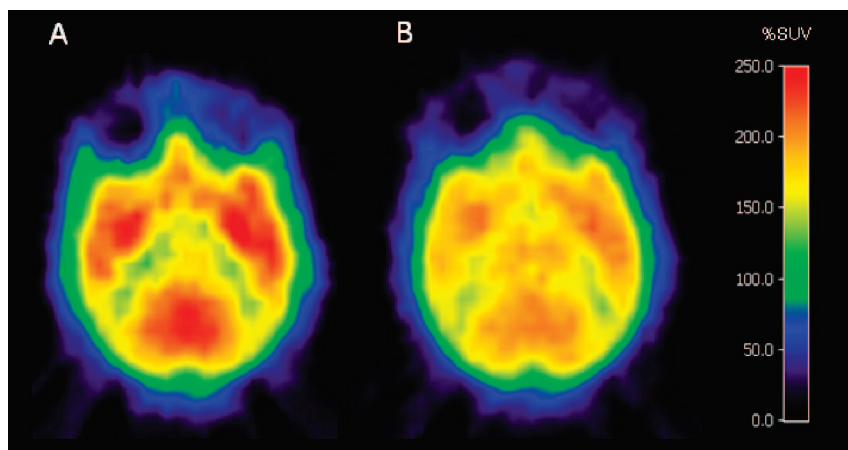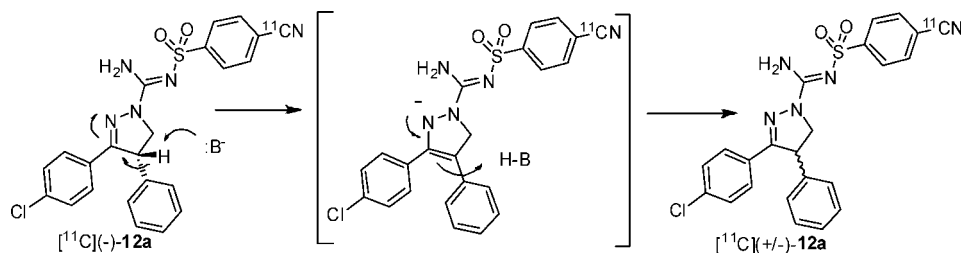

Figure 5. Horizontal PET images, obtained at the level of the striatum from data acquired between 9 and 93 min after injection of $[^{11}C](-)$-**12a** (100 MBq, (A)) or $[^{11}C](+)$-**12a** (98 MBq, (B)).

Scheme 3. Proposed Mechanism for the Epimerization of $[^{11}C](-)$-**12a** under Labeling Conditions

MD). Specific rotations were obtained at room temperature. Mass spectra (MS) were acquired using a LCQ^{DECA} LC-MS instrument (Thermo Finnigan, San Jose, CA) fitted with a reverse phase LC column (Luna, C18; 5 μm, 2 mm × 150 mm; Phenomenex). Radiosyntheses were performed in a custom-made remotely controlled apparatus.[38] Radioligand separations were performed with HPLC on a reverse phase column (μ-Bondapak C-18; 7.8 mm ×

300 mm, 10 μm; Waters). The column outlet was connected to an absorbance detector ($\lambda = 254$ nm) in series with a GM-tube for radiation detection. $[^{11}C](\pm)$-**12a**, $[^{11}C](-)$-**12a**, and $[^{11}C](+)$-**12a** were purified in this system using MeCN-0.01 M H_3PO_4 (55: 45, v/v) as mobile phase at 6 mL/min. The radiochemical purities and specific radioactivities of each product were determined with reverse phase HPLC on a μ-Bondapak C-18 column (3.9 mm × 300 mm,
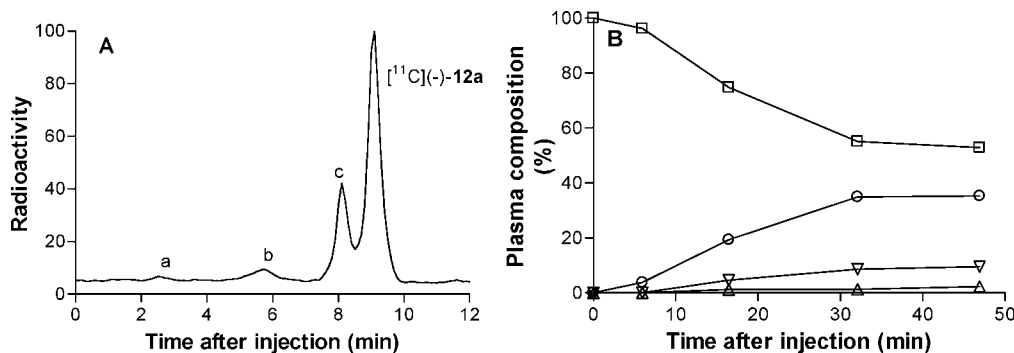
Figure 6. Radio-HPLC of plasma of $[^{11}C](-)$-**12a** in cynomolgus monkeys at 15 min after injection (A), and time course of radioactivity in plasma represented by parent radioligand and radiometabolite fractions (B). Key: □, $[^{11}C](-)$-**12a**; △, metabolite a; ▽, metabolite b; ○, metabolite c.

10 μm; Waters) eluted at 3 mL/min with MeCN-H₃PO₄ (0.01 M; 55: 45 v/v) as mobile phase. Eluate was monitored with an absorbance detector (λ = 254 nm) in series with a β-flow detector (Beckman) for radiation detection. The enantiomeric excess of each labeled product was measured by chiral HPLC, as described above; eluate was monitored for absorbance and radioactivity. Specific radioactivities (GBq/μmol) were determined with analytical HPLC calibrated for absorbance (λ = 254 nm) response per mass of ligand. The specific radioactivity was calculated as the radioactivity of the radioligand peak (decay-corrected) (GBq) divided by the mass of the associated carrier peak (μmol). The metabolism of $[^{11}C](-)$-**12a** was assessed with HPLC on a reverse phase (μ-Bondapak C-18 column; 7.8 mm × 300 mm, 10 μm; Waters) eluted at 6 mL/min with a gradient of MeCN (A) and aq-H₃PO₄ (0.01 M) (B), with A increasing linearly from 35 to 65% v/v for 6 min and then to 35% v/v over the next 2 min and then held for 4 min. The column outlet was connected to an absorbance detector (λ = 270 nm) in series with a GM-tube for radiation detection.

N-[(4-Cyanophenyl)sulfonyl]carbamic acid methyl ester (10a). Methyl chloroformate (6.34 mL, 82.4 mmol) was slowly added to a stirred solution of 4-cyanobenzenesulfonamide (10 g, 54.9 mmol) and triethylamine (23 mL, 165 mmol) in acetonitrile (75 mL). The reaction was stirred at room temperature for 16 h and then evaporated to dryness in vacuo. After addition of ethyl acetate and aq NaHCO₃ to the crude residue, the aqueous layer was separated and acidified. The oily precipitate crystallized on standing and was filtered off, washed with water, and dried to give **10a** (6.9 g, 52% yield); mp 130−132 °C. ¹H NMR (400 MHz, CDCl₃): δ 3.72 (s, 3H), 7.87 (2H, dt, J = 9.0, 2.0 Hz), 8.19 (2H, dt, J = 8.8, 2.0 Hz), NH proton invisible.

N-[(4-Bromophenyl)sulfonyl]carbamic acid methyl ester (10b). **10b** was prepared from 4-bromobenzenesulfonamide in 48% yield by the method described for **10a**; mp 120−122 °C. ¹H NMR (400 MHz, CDCl₃): δ 3.72 (s, 3H), 7.71 (2H, dt, J = 8.8, 2.0 Hz), 7.93 (2H, dt, J = 8.8, 2.0 Hz), NH proton invisible.

N-[(4-Iodophenyl)sulfonyl]carbamic acid methyl ester (10c). **10c** was prepared from 4-iodobenzenesulfonamide in 56% yield by the method described for **10a**; mp 116−118 °C. ¹H NMR (400.13 MHz, CDCl₃): δ 3.72 (s, 3H), 7.77 (2H, dt, J = 8.8, 2.0 Hz), 7.93 (2H, dt, J = 8.8, 2.0 Hz), NH proton invisible.

3-(4-Chlorophenyl)-N-[(4-cyanophenyl)sulfonyl]-4-phenyl-4,5-dihydro-1H-pyrazole-1-carboxamide (11a). To a solution of 3-(4-chlorophenyl)-4,5-dihydro-4-phenyl-1H-pyrazole (6.4 g, 25.4 mmol) in toluene (100 mL) was added **10a** (6.1 g, 25.4 mmol), and the resulting solution was heated to reflux for 2 h. After cooling to room temperature, **11a** began to crystallize slowly from solution. The crystals were filtered off and washed twice with MTBE to give pure **11a** (9.2 g, 78% yield); mp 208−210 °C. ¹H NMR (400 MHz, CDCl₃): δ 3.92 (1H, dd, J = 6.2, 5.2 Hz), 4.34 (1H, t, J = 4.3 Hz), 4.75 (1H, dd, J = 6.2, 5.2 Hz), 7.12 (2H, dt, J = 6.6, 1.6 Hz), 7.33−7.24 (5H, m), 7.55 (2H, dt, J = 8.6, 1.8 Hz), 7.86 (2H, dt, J = 8.6, 1.8 Hz), 8.30 (2H, dt, J = 8.6, 1.8 Hz), 8.8 (1H, bs). ¹³C NMR (100 MHz, CDCl₃): δ 51.54, 54.02, 117.39, 127.21, 127.92,

128.25, 128.74, 129.08, 129.23, 129.61, 132.72, 136.85, 138.93, 143.06, 147.55, 156.82. LC-MS m/z (M⁺ + H) = 464.9. HRMS calcd for C₂₃H₁₈N₄O₃SCl (M⁺ + H), 465.0788; found, 465.0774; error (ppm): −3.0.

3-(4-Chlorophenyl)-N-[(4-bromophenyl)sulfonyl]-4-phenyl-4,5-dihydro-1H-pyrazole-1-carboxamide (11b). **11b** was prepared from 3-(4-chlorophenyl)-4,5-dihydro-4-phenyl-1H-pyrazole and **10b** in 82% yield by the method described for **11a**; mp 214−216 °C. ¹H NMR (400 MHz, CDCl₃): δ 3.92 (1H, dd, J = 6.2, 5.2 Hz), 4.34 (1H, t, J = 4.3 Hz), 4.75 (1H, dd, J = 6.2, 5.2 Hz), 7.12 (2H, dt, J = 6.6, 1.6 Hz), 7.33−7.24 (5H, m), 7.55 (2H, dt, J = 8.6, 1.8 Hz), 7.71 (2H, dt, J = 8.6, 1.8 Hz), 8.04 (2H, dt, J = 8.6, 1.8 Hz), 8.76 (1H, s). ¹³C NMR (100.62 MHz, DMSO-d_6): δ 21.02, 49.43, 54.53, 101.86, 125.28, 127.25, 127.48, 128.17, 128.56, 128.87, 129.06, 129.17, 129.26, 134.69, 137.31, 137.92, 138.16, 139.59, 140.15, 148.52, 155.89. LC-MS m/z (M⁺ + H) = 519.9. HRMS calcd for C₂₂H₁₈N₃O₃SClBr (M⁺ + H), 517.9941; found 517.9929; error (ppm): −2.3.

3-(4-Chlorophenyl)-N-[(4-iodophenyl)sulfonyl]-4-phenyl-4,5-dihydro-1H-pyrazole-1-carboxamide (11c). **11c** was prepared from 3-(4-chlorophenyl)-4,5-dihydro-4-phenyl-1H-pyrazole and **10c** in 74.5% yield by the method described for **11a**; mp 212−214 °C. ¹H NMR (400 MHz, CDCl₃): δ 3.92 (1H, dd, J = 6.2, 5.2 Hz), 4.34 (1H, t, J = 4.3 Hz), 4.73 (1H, dd, J = 6.1, 5.2 Hz), 7.16 (2H, dt, J = 6.6, 1.6 Hz), 7.33−7.24 (5H, m), 7.55 (2H, dt, J = 8.7, 2.0 Hz), 7.71 (4H, qt, J = 9.8, 8.8, 1.8 Hz), 8.8 (1H, s). ¹³C NMR (100.62 MHz, CDCl₃): δ 51.5, 54.0, 127.2, 128.1, 128.2, 128.3, 128.7, 129.1, 129.6, 129.9, 132.3, 136.7, 138.1, 139.1, 147.8, 156.4. LC-MS m/z (M⁺ + H) = 565.8. HRMS calcd for C₂₂H₁₈N₃O₃SClI (M⁺ + H), 565.9802; found: 565.9801; error (ppm): −0.2.

3-(4-Chlorophenyl)-N′-[(4-cyanophenyl)sulfonyl]-4-phenyl-4,5-dihydro-1H-pyrazole-1-carboxamidine (12a). A mixture of **11a** (6 g, 12.9 mmol) and PCl₅ (2.8 g, 13.5 mmol) was dissolved in chlorobenzene (80 mL), refluxed for 1 h, and then concentrated in vacuo. The residue was treated with methanolic NH₃ (1M, 35 mL). The mixture was stirred at room temperature for 1 h and then concentrated in vacuo. The product was recrystallized from MeOH to give **12a** (2.2 g, 37%); mp 208−210 °C. ¹H NMR (400.13 MHz, CDCl₃): δ 4.02 (dd, J = 12.0, 4.0 Hz, 1H), 4.42 (t, J = 12.0 Hz, 1H), 4.76 (dd, J = 12.0, 4.0 Hz, 1H), 7.10 (dt, J = 6.4, 2.0 Hz, 2H), 7.34−2.25 (m, 3H), 7.55 (dt, J = 8.7, 2.0 Hz, 2H), 7.6 (d, J = 8.0 Hz, 2H), 7.75 (dt, J = 8.6, 1.4 Hz, 2H), 8.05 (dt, J = 8.6, 1.4 Hz, 2H). ¹³C NMR (100.62 MHz, CDCl₃): δ 51.42, 55.34, 115.29, 117.77, 126.87, 127.18, 128.04, 128.22, 128.69, 129.09, 129.61, 132.58, 136.89, 138.93, 147.60, 152.72, 158.05. LC-MS m/z (M⁺ + H), 464.0. HRMS calcd for C₂₃H₁₉N₅O₂SCl (M⁺ + H), 464.0948; found; 464.0957; error (ppm): 1.9.

(−)-3-(4-Chlorophenyl)-N′-[(4-cyanophenyl)sulfonyl]-4-phenyl-4,5-dihydro-1H-pyrazole-1-carboxamidine ((−)-12a). Resolution of **12a** by chiral HPLC (see General Methods) gave (−)-**12a** (t_R = 9.8 min at 8 mL/min; >98% ee); $[\alpha]_D^{22}$ = −69.3°, c = 0.010, CH₂Cl₂; mp 208−210 °C. ¹H NMR: as found for **12a**. MS m/z (M⁺ + H), 464.1. HRMS, calcd for C₂₃H₁₉N₅O₂SCl (M⁺ + H),

464.0948; found, 464.0962; error (ppm): 3.0. Anal. ($C_{23}H_{18}$-ClN_5O_2S) C, H, N.

(+)-3-(4-Chlorophenyl)-*N*′-[(4-cyanophenyl)sulfonyl]-4-phenyl-4,5-dihydro-1*H*-pyrazole-1-carboxamidine ((+)-12a). Resolution of **12a** by chiral HPLC (see General Methods) gave (+)-**12a** (t_R = 12.27 min at 8 mL/min, >98% ee; $[\alpha]_D^{22}$ = + 66.3°, c = 0.011, CH_2Cl_2; mp 208−210 °C. ^{1}H NMR: as found for **12a**. MS *m/z* (M$^+$ + H) 464.1. HRMS calcd for $C_{23}H_{19}N_5O_2SCl$ (M$^+$ + H) 464.0948; found, 464.0961, error (ppm): 2.8. Anal. ($C_{23}H_{18}$-ClN_5O_2S) C, H, N.

3-(4-Chlorophenyl)-*N*′-[(4-bromophenyl)sulfonyl]-4-phenyl-4,5-dihydro-1*H*-pyrazole-1-carboxamidine (12b). **12b** was prepared from **11b** in 43% yield by the method described for **12a**; mp 214−216 °C. ^{1}H NMR (400.13 MHz, DMSO-d_6): δ 3.80 (1H, dd, J = 6.6, 4.7 Hz), 4.37 (1H, t, J = 11.5 Hz), 5.04 (1H, dd, J = 6.6, 4.7 Hz), 7.16 (2H, d, J = 7.1 Hz), 7.25 (1H, t, J = 7.2 Hz), 7.35 (2H, t, J = 7.6 Hz), 7.44 (2H, d, J = 8.6 Hz), 7.76 (2H, d, J = 8.4 Hz), 7.79−7.71 (2H, m). ^{13}C NMR (100.62 MHz, DMSO-d_6) δ 49.62, 55.60, 125.22, 127.20, 127.52, 127.85, 128.60, 128.83, 129.12, 129.21, 131.83, 134.92, 140.05, 142.96, 152.76, 157.60. LC-MS *m/z* [M + H]$^+$ 517.0; HRMS calcd for $C_{22}H_{19}N_4O_2SClBr$ (M$^+$ + H), 517.0101; found, 517.0117, error (ppm): 3.1.

(−)-3-(4-Chlorophenyl)-*N*′-[(4-bromophenyl)sulfonyl]-4-phenyl-4,5-dihydro-1*H*-pyrazole-1-carboxamidine ((−)-12b). Resolution of **12b** by chiral HPLC (see General Methods) gave (−)-**12b** (t_R = 13.78 min at 8 mL/min, >98% ee); $[\alpha]_D^{22}$ = −65.7°, c = 0.010, CH_2Cl_2; mp 214−216 °C. ^{1}H NMR: as found for **12b**. MS *m/z* (M$^+$ + H) 517.0. HRMS calcd for $C_{22}H_{19}N_4O_2SClBr$ (M$^+$ + H) 517.0101, found: 517.0126, error (ppm): 4.8.

(+)-3-(4-Chlorophenyl)-*N*′-[(4-bromophenyl)sulfonyl]-4-phenyl-4,5-dihydro-1*H*-pyrazole-1-carboxamidine ((+)-12b). Resolution of **12b** by chiral HPLC (see General Methods) gave (+)-**12b** (t_R = 18.14 min at 8 mL/min, >98% ee); $[\alpha]_D^{22}$ = 65.2°, c = 0.010, CH_2Cl_2; mp 214−216 °C. ^{1}H NMR: as found for **12b**. MS *m/z* (M$^+$ + H) 517.0. HRMS calcd for $C_{22}H_{19}N_4O_2SClBr$ (M$^+$ + H) 517.0101, found: 517.0110, error (ppm): 1.7.

3-(4-Chlorophenyl)-*N*′-[(4-iodophenyl)sulfonyl]-4-phenyl-4,5-dihydro-1*H*-pyrazole-1-carboxamidine (12c). **12c** was prepared from **11c** in 64% yield by the method described for **12a**; mp 222−224 °C. ^{1}H NMR (400 MHz, DMSO-d_6): δ 3.80 (1H, dd, J = 6.6, 4.7 Hz), 4.37(1H, t, J = 11.5 Hz), 5.04 (1H, dd, J = 6.6, 4.7 Hz), 7.18 (2H, d, J = 7.1 Hz), 7.26 (1H t, J = 7.2 Hz), 7.35 (2H, t, J = 7.6 Hz), 7.44 (2H, d, J = 8.6 Hz), 7.62 (2H, d, J = 8.4 Hz), 7.77 (2H, d, J = 8.6 Hz), 7.90 (2H, d, J = 8.4 Hz). ^{13}C NMR (100.62 MHz, DMSO-d_6): δ 49.60, 55.59, 99.28, 127.19, 127.52, 127.59, 128.69, 128.83, 129.11, 129.21, 134.92, 137.65, 140.05, 143.30, 152.74, 157.57. LC-MS *m/z* (M$^+$ + H) 565.1. HRMS calcd for $C_{22}H_{19}N_4O_2SClI$ (M$^+$ + H) 564.9962, found, 564.9974, error (ppm): 2.1.

(−)-3-(4-Chlorophenyl)-*N*′-[(4-iodophenyl)sulfonyl]-4-phenyl-4,5-dihydro-1*H*-pyrazole-1-carboxamidine ((−)-12c). Resolution of **12c** by chiral HPLC (see General Methods) gave (−)-**12c** (t_R = 18.18 min at 6 mL/min, >98% ee); $[\alpha]_D^{22}$= −160°, c = 0.011, CHCl$_3$; mp 222−224 °C. ^{1}H NMR: as found for **12c**. LC-MS *m/z* (M$^+$ + H) 565.1. HRMS calcd for $C_{22}H_{19}N_4O_2SClI$ (M$^+$ + H): 564.9962, found: 564.9960, error (ppm): −0.4. Anal. ($C_{22}H_{18}ClIN_4O_2S$) C, H, N.

(+)-3-(4-Chlorophenyl)-*N*′-[(4-iodophenyl)sulfonyl]-4-phenyl-4,5-dihydro-1*H*-pyrazole-1-carboxamidine ((+)-12c). Resolution of **12c** by chiral HPLC (see General Methods) gave (+)-**12c** (t_R = 24.38 min at 6 mL/min, >98% ee); $[\alpha]_D^{22}$ = + 151°, c = 0.010, CHCl$_3$; mp 222−224 °C. ^{1}H NMR: as found for **12c**. LC-MS *m/z* (M$^+$ + H) 565.0. HRMS calcd for $C_{22}H_{19}N_4O_2SClI$ (M$^+$ + H) 564.9962, found, 564.9960, error (ppm): −0.4. Anal. ($C_{22}H_{18}ClIN_4O_2S$) C, H, N.

CB$_1$ and CB$_2$ Binding Assays. Frozen cell membranes (recombinant hCB1r or hCB2r; Perkin-Elmer) were thawed and diluted (7 µg/well) in membrane buffer (final concentrations: 100 mM NaCl, 5 mM MgCl$_2$, 1 mM EDTA, 50 mM HEPES, 10 µM GDP, 100 µM DTT, 0.01% fatty acid free BSA).

[^{35}S]GTPγS was diluted with distilled water to a final concentration of 0.5 nM. The inhibitory effect of test ligands was measured against a concentration (EC$_{80}$) of the CB1r/CB2r agonist CP-55940 (Tocris) added to the solution.

Membrane solution (100 µL) and radioligand solution (100 µL) were added to the assay plates together with 2 µL compound (concentration-response in DMSO) and incubated for 45 min at 30 °C. Bound [^{35}S]GTPγS was separated from free [^{35}S]GTPγS by rapid filtration under vacuum through Whatman GF/B glass fiber filters, followed by washes with cold wash solution (final concentration: 50 mM Tris, 5 mM MgCl$_2$, 50 mM NaCl). The filters were dried for 60 min at 50 °C. Scintillation film was melted onto the filters, which were then counted in a Microbeta scintillation counter. Nonspecific binding was determined in the presence of a saturating concentration of GTPγS (final concentration 20 µM). IC$_{50}$ values were converted to K_i values according to the Cheng and Prusoff equation.[39] The data represent K_i ± SD (nM) from triplicate determinations vs CB1r or CB2r.

Receptor Screening. Ligand (−)-**12a** was screened for binding to a wide range of receptors and transporters by the National Institute of Mental Health Psychoactive Drug Screening Program. Detailed protocols are available online for all binding assays at the NIMH-PDSP Web site (http://pdsp.med.unc.edu).

[^{11}C]HCN Production. [^{11}C]Methane was produced at the Karolinska Hospital with a GEMS PETtrace cyclotron using 16.4 MeV protons in the ^{14}N(p,α)^{11}C reaction on N$_2$(g) containing 10% H$_2$(g).[40] The target gas was irradiated for 5 min with a beam intensity of 35 µA. The [^{11}C]methane was isolated from the target gas in a Porapak Q trap, which was cooled with N$_2$(l). The Porapak Q trap was warmed and the [^{11}C]methane passed in nitrogen (200 mL/min) with NH$_3$(g) (20−30 mL/min) over heated (990 °C) Pt wire (1.3 g, 0.127 mm, 99%; Sigma Aldrich) in a quartz tube within a Carbolite furnace (MTF 10/15). The resulting [^{11}C]NH$_4$CN was bubbled through aq 50% H$_2$SO$_4$ (2 mL) at 56 °C to generate [^{11}C]HCN.

Radiosyntheses of [^{11}C](±)-12a, [^{11}C](−)-12a, and [^{11}C](+)-12a. The generated [^{11}C]HCN (∼12.4 GBq) was trapped in a V-vial (5-mL) containing DMSO (400 µL) base (KOH, 1 mg, 17.8 µmol; K 2.2.2, 5 mg, 13.3 µmol) for [^{11}C](±)-**12a** or KH$_2$PO$_4$ (1 mg, 7.34 µmol) for [^{11}C](−)-**12a** or [^{11}C](+)-**12a**. After trapping of [^{11}C]HCN was complete, the solution was transferred into another V-vial (10 mL) which contained DMSO (400 µL), Pd(PPh$_3$)$_4$ (5.5 mg, 4.8 µmol) and the requisite precursor ((±)-**12b**, (−)-**12b**, (−)-**12c**, or (+)-**12c**; 1 mg). The reaction was heated 135 °C for 4 min and then cooled to room temperature. HPLC mobile phase (800 µL) was added to the V-vial and the radioactive product separated with HPLC (see General Methods). The radioactive fraction (t_R = 12.3 min) was collected, evaporated to dryness, and taken up in ethanol-propylene glycol (30:70 v/v, 3 mL) with sterile phosphate buffer (0.2 M, pH = 7.4, 5 mL) and filtered through a sterile filter (Millex GV, 0.22 µm pore size; Millipore Corp., Corrigtwohill, Co. Cork, Ireland).[41] A sample (∼100 µL) was analyzed by HPLC for radiochemical purity and measurement of specific radioactivity (see General Methods).

PET Measurements in Monkey. Cynomolgus monkey (*Macaca fascicularis*) experiments were performed at the Karolinska Institutet (KI) according to "Guidelines for Planning, Conducting and Documenting Experimental Research" (Dnr 4820/06-600) of the KI as well as the "Guide for the Care and Use of Laboratory Animals".[42] The study was approved by the Animal Ethics Committee of the Swedish Animal Welfare Agency. Two cynomolgus monkeys (3.4 and 4.8 kg) were used in the PET experiments. Anesthesia was induced and maintained with repeated im injections of a mixture of ketamine hydrochloride (3.75 mg/kg^{-1} h^{-1} Ketalar, Pfizer) and xylazine hydrochloride (1.5 mg/kg^{-1} h^{-1} Rompun Vet., Bayer). The head for each monkey was immobilized in a stereotactic frame for the duration of scans.[43] The body temperature was maintained by a Bair Hugger model 505 (Arizant Healthcare, MN) and monitored by rectal thermometer (Precision Thermometer, Harvard Apparatus, MA).

In baseline experiments, each radioligand was administered by bolus injection over about 5 s, with injected activities of 56, 100, and 98 MBq and specific radioactivities of 78, 65, and 56 GBq/μmol for [^{11}C]($\pm$)-**12a**, [^{11}C]($-$)-**12a**, and [^{11}C]($+$)-**12a**, respectively. The masses of injected carrier ligand were 0.33 μg (0.72 nmol), 0.71 μg (1.53 nmol), and 0.81 μg (1.75 nmol) for [^{11}C]($\pm$)-**12a**, [^{11}C]($-$)-**12a**, and [^{11}C]($+$)-**12a**. In the displacement experiment, **6** (1 mg/kg, iv) was infused at 25 min after injection of [^{11}C]($\pm$)-**12a**. For this purpose, compound **6** was formulated in vehicle solution (8 mL) (saline/alcohol/cremophore EL, 9:1:0.1 by vol.). The solution was homogenized by vortexing and then passed through a sterile filter (0.2 μm pore size, Millex-GV, Millipore). The injected activity was 56 MBq with a specific radioactivity of 80.3 GBq/μmol. The mass of carrier associated with the injected radioactivity was 0.32 μg (0.70 nmol). The preblock experiment was performed at 5 h after the baseline experiment. **6** was infused at 20 min before injection of radioligand. The injected activity was 57 MBq with specific radioactivities of 75.4 GBq/μmol. The mass of carrier associated with the injected radioactivity was 0.35 μg (0.76 nmol). In each PET experiment, scans were acquired in 3 frames over 93 min.

PET Imaging. Radioactivity in brain was measured with the Siemens ECAT EXACT HR system. The three-ring detector block architecture gives a 15-cm wide field of view. All acquisitions were acquired in 3D-mode.[44] The transversal resolution in the reconstructed image is about 3.8 mm full-width half-maximum (fwhm) and the axial resolution, 3.125 mm. The data were corrected for attenuation with three rotating ^{68}Ge rod sources. Raw PET data were then reconstructed using standard filtered back projection consisting of the following reconstruction parameters: 2 mm Hanning filter, scatter correction, a zoom factor of 2.17, and a 128 × 128 matrix size.[44] Emission data were collected continuously for 93 min, according to a preprogrammed series of 20 frames starting immediately after iv injection of radioligand. The 3 initial frames were 1 min each, followed by 4 frames of 3 min each and 13 frames of 6 min each.

The mean image of the PET measurements (9−93 min) was transformed into a standard anatomical space using the monkey version of the Human Brain Atlas developed at the Karolinska Institutet.[45] The transformation matrix generated on this image was applied to all frames of the corresponding baseline, displacement, and pretreatment experiments. PET data were subsequently resliced to a resolution of 1.00, 1.00, 1.00 mm. Volumes of interest (VOIs) were manually defined on the coronal planes of an average monkey MRI. Similar VOIs were applied, as reported by Yasuno et al.,[29] including cerebellum (1.9 cm³), frontal cortex (7.4 cm³), lateral temporal cortex (5.0 cm³), medial temporal cortex (2.9 cm³), striatum (2.1 cm³), thalamus (0.9 cm³), and pons (0.7 cm³). Tissue radioactivity concentrations were expressed as % standardized uptake values (%SUV). Tissue radioactivity concentrations were decay-corrected and, in order to normalize for injected dose and body weight, expressed as % standardized uptake values (%SUV), where:

$$\%\text{SUV} = \left[\frac{\% \text{ injected activity}}{\text{brain tissue (g)}} \times \text{body weight (g)} \right] \quad (1)$$

PET Plasma Measurements. For radiometabolite measurements, venous blood (1 mL) was sampled from monkey at 5, 15, 30, and 45 min after injection of each radioligand. Plasma samples were measured as described previously.[46] Briefly, the supernatant liquid (0.5 mL) obtained after centrifugation at 2000g for 1 min was mixed with MeCN (0.7 mL) containing standard ($\pm$)-**12a**. The supernatant liquid (1 mL) after another centrifugation at 2000g for 1 min was counted in a well counter and subsequently injected onto HPLC.

Supporting Information Available: Table of elemental analyses for target ligands ($-$)-**12a**, ($+$)-**12a**, ($-$)-**12c**, and ($+$)-**12c.** This material is available free of charge via Internet at http://pubs.acs.org.

References

(1) Vincent, B. J.; McQuiston, D. J.; Einhorn, L. H.; Nagy, C. M.; Brames, M. J. Review of cannabinoids and their anti-emetic effectiveness. *Drugs* **1983**, *25*, 52–62.

(2) Mackie, K. Cannabinoid receptors as therapeutic targets. *Annu. Rev. Pharmacol. Toxicol.* **2005**, *46*, 101–122.

(3) Lambert, D. M.; Fowler, C. J. The endocannabinoid system: drug targets, lead compounds, and potential therapeutic applications. *J. Med. Chem.* **2005**, *48*, 5059–5087.

(4) Izzo, A. A.; Coutts, A. A. Cannabinoids and the digestive tract. *Handb. Exp. Pharmacol.* **2005**, *168*, 573–598.

(5) Darmani, N. A.; Crim, J. L. Δ^9-Tetrahydrocannibinol differentially suppresses emesis versus enhanced locomotor activity produced by chemically diverse dopamine D_2/D_3 receptor agonists in the least shrew (*Cryptotis parva*). *Pharmacol., Biochem. Behav.* **2005**, *80*, 35–44.

(6) Beal, J. E.; Olson, R.; Laubenstein, L.; Morales, J. O.; Bellman, P.; Yangco, B.; Lefkowitz, L.; Plasse, T. F.; Shepard, K. V. Dronabinol as a treatment for anorexia associated with weight loss in patients with AIDS. *J. Pain Symptom Manage.* **1995**, *10*, 89–97.

(7) Beal, J. E.; Olson, R.; Lefkowitz, L.; Laubenstein, L.; Bellman, P.; Yangco, B.; Morales, J. O.; Murphy, R.; Powderly, W.; Plasse, T. F.; Mosdell, K. W.; Shepard, K. V. Long-term efficacy and safety of dronabinol for acquired immunodeficiency syndrome-associated anorexia. *J. Pain Symptom Manage.* **1997**, *14*, 7–14.

(8) Grundy, R. I. The therapeutic potential of the cannabinoids in neuroprotection. *Expert Opin. Investig. Drugs* **2002**, *11*, 1365–1374.

(9) Pryce, G.; Ahmed, Z.; Hankey, D. J.; Jackson, S. J.; Croxford, J. L.; Pocock, J. M.; Ledent, C.; Petzold, A.; Thompson, A. J.; Giovannoni, G.; Cuzner, M. L.; Baker, D. Cannabinoids inhibit neurodegeneration in models of multiple sclerosis. *Brain* **2003**, *126*, 2191–2202.

(10) Gaoni, Y.; Mechoulam, R. Isolation structure and partial synthesis of active constituent of hashish. *J. Am. Chem. Soc.* **1964**, *86*, 1646–1647.

(11) Mechoulam, R.; Gaoni, Y. The absolute configuration of Δ^1-tetrahydrocannibinol, the major active constituent of hashish. *Tetrahedron. Lett.* **1967**, *12*, 1109–1111.

(12) Devane, W. A.; Dysarz, F. A.; Johnson, M. R.; Melvin, L. S.; Howlett, A. C. Determination and characterization of a cannabinoid receptor in rat-brain. *Mol. Pharmacol.* **1988**, *34*, 605–613.

(13) Munro, S.; Thomas, K. L.; Abushaar, M. Molecular characterization of a peripheral receptor for cannabinoids. *Nature* **1993**, *365*, 61–65.

(14) Shire, D.; Carillon, C.; Kaghad, M.; Calandra, B.; Rinaldicarmona, M.; Lefur, G.; Caput, D.; Ferrara, P. An amino-terminal variant of the central cannabinoid receptor resulting from alternative splicing. *J. Biol. Chem.* **1995**, *270*, 3726–3731.

(15) Ryberg, E.; Vu, H. K.; Larsson, N.; Groblewski, T.; Hjorth, S.; Elebring, T.; Sjorgren, S.; Greasley, P. J. Identification and characterisation of a novel splice variant of the human CB_1 receptor. *FEBS Lett.* **2005**, *579*, 259–264.

(16) Herkenham, M.; Lynn, A. B.; Little, M. D.; Johnson, M. R.; Melvin, L. S.; Decosta, B. R.; Rice, K. C. Cannabinoid receptor localization in brain. *Proc. Natl. Acad. Sci. U.S.A.* **1990**, *87*, 1932–1936.

(17) Herkenham, M.; Lynn, A. B.; Johnson, M. R.; Melvin, L. S.; Decosta, B. R.; Rice, K. C. Characterization and localization of cannabinoid receptors in rat brain: a quantitative in vitro autoradiographic study. *J. Neurosci.* **1991**, *11*, 563–583.

(18) Lynn, A. B.; Herkenham, M. Localization of cannabinoid receptors and nonsaturable high-density cannabinoid binding sites in peripheral tissues of the rat: implications for receptor-mediated immune modulation by cannabinoids. *J. Pharmacol. Exp. Ther.* **1994**, *268*, 1612–1623.

(19) Griffin, G.; Fernando, S. R.; Ross, R. A.; McKay, N. G.; Ashford, M. L. J.; Shire, D.; Huffman, J. W.; Yu, S.; Lainton, J. A. H.; Pertwee, R. G. Evidence for the presence of CB_2-like cannabinoid receptors on peripheral nerve terminals. *Eur. J. Pharmacol.* **1997**, *339*, 53–61.

(20) Rinaldi-Carmona, M.; Barth, F.; Heaulme, M.; Shire, D.; Calandra, B.; Congy, C.; Martinez, S.; Maruani, J.; Neliat, G.; Caput, D.; Ferrara, P.; Soubrié, P.; Brelière, J.-C.; Le Fur, G. SR141716A, a potent and selective antagonist of the brain cannabinoid receptor. *FEBS Lett.* **1994**, *350*, 240–244.

(21) Lange, J. H. M.; Kruse, C. G.; Tipker, J.; Tulp, M. T. M.; Van Vliet, B. J. 4,5-Dihydro-1*H*-pyrazole derivatives having CB₁-antagonist activity. PTC Int. Appl. WO 0170700, 2001.

(22) Lange, J. H. M.; Coolen, H.; van Stuivenberg, H. H.; Dijksman, J. A. R.; Herremans, A. H. J.; Ronken, E.; Keizer, H. G.; Tipker, K.; McCreary, A. C.; Veerman, W.; Wals, H. C.; Stork, B.; Verveer, P. C.; den Hartog, A. P.; de Jong, N. M. J.; Adolfs, T. J. P.; Hoogendoorn, J.; Kruse, C. G. Synthesis, biological properties, and molecular modeling investigations of novel 3,4-diarylpyrazolines as potent and selective CB₁ cannabinoid receptor antagonists. *J. Med. Chem.* **2004**, *47*, 627–643.

(23) Lange, J. H. M.; Kruse, C. G.; Tipker, J.; Hoogendoorn, J. 4,5-Dihydro-1H-pyrazole derivatives having CB₁-antagonist activity. PTC Int. Appl. WO 02076949, 2002.

(24) Horti, A. G.; Fan, H.; Kuwabara, H.; Hilton, J.; Ravert, H. T.; Holt, D. P.; Alexander, M.; Kumar, A.; Rahmim, A.; Scheffel, U.; Wong, D. F.; Dannals, R. F. ¹¹C-JHU75528: A radiotracer for PET imaging of CB₁ cannabinoid receptors. *J. Nucl. Med.* **2006**, *47*, 1689–1696.

(25) Fan, H.; Ravert, H. T.; Holt, D. P.; Dannals, R. F.; Horti, A. G. Synthesis of 1-(2,4-dichlorophenyl)-4-cyano-5-(4-[¹¹C]methoxyphenyl)-*N*-(piperidin-1-yl)-1*H*-pyrazole-3-carboxamide ([¹¹C]JHU75528) and 1-(2-bromophenyl)-4-cyano-5-(4-[¹¹C]methoxyphenyl)-*N*-(piperidin-1-yl)-1*H*-pyrazole-3-carboxamide ([¹¹C]JHU75575) as potential radioligands for PET imaging of cerebral cannabinoid receptor. *J. Label. Compd. Radiopharm.* **2006**, *49*, 1021–1036.

(26) Donohue, S. R.; Halldin, C.; Schou, M.; Hong, J.; Phebus, L. A.; Chernet, E.; Hitchcock, S. A.; Gardinier, K. M.; Ruley, K. M.; Krushinski, J. H.; Schaus, J. M.; Pike, V. W. Radiolabeling of a high potency cannabinoid subtype-1 receptor ligand, *N*-(4-fluoro-benzyl)-4-(3-(piperidin-1-yl)-indole-1-sulfonyl)benzamide (PipISB), with carbon-11 or fluorine-18. *J. Label. Compd. Radiopharm.* **2008**, *51*, 146–152.

(27) Burns, H. D.; Van Laere, K.; Sanabria-Bohorquez, S.; Hamill, T. G.; Bormans, G.; Eng, W. S.; Gibson, R.; Ryan, C.; Connolly, B.; Patel, S.; Krause, S.; Vanko, A.; Van Hecken, A.; Dupont, P.; De Lepeleire, I.; Rothenberg, P.; Stoch, S. A.; Cote, J.; Hagmann, W. K.; Jewell, J. P.; Lin, L. S.; Liu, P.; Goulet, M. T.; Gottesdiener, K.; Wagner, J. A.; de Hoon, J.; Mortelmans, L.; Fong, T. M.; Hargreaves, R. J. [¹⁸F]MK-9470, a positron emission tomography (PET) tracer for in vivo human PET brain imaging of the cannabinoid-1 receptor. *Proc. Natl. Acad. Sci. U.S.A.* **2007**, *104*, 9800–9805.

(28) Liu, P.; Lin, L. S.; Hamill, T. G.; Jewell, J. P.; Lanza, T. J.; Gibson, R. E.; Krause, S. M.; Ryan, C.; Eng, W. S.; Sanabria, S.; Tong, X. C.; Wang, J. Y.; Levorse, D. A.; Owens, K. A.; Fong, T. M.; Shen, C. P.; Lao, J.; Kumar, S.; Yin, W. J.; Payack, J. F.; Springfield, S. A.; Hargreaves, R.; Burns, H. D.; Goulet, M. T.; Hagmann, W. K. Discovery of *N*-{(1S,2S)-2-(3-Cyanophenyl)-3-[4-(2-[¹⁸F]fluoroethoxy)phenyl]-1-methylpropyl}-2-methyl-2-[(5-methylpyridin-2-yl)oxy]propanamide, a cannabinoid-1 receptor positron emission tomography tracer suitable for clinical use. *J. Med. Chem.* **2007**, *50*, 3427–3430.

(29) Yasuno, F.; Brown, A. K.; Zoghbi, S. S.; Krushinski, J. H.; Chernet, E.; Tauscher, J.; Schaus, J. M.; Phebus, L. A.; Chesterfield, A. K.; Felder, C. C.; Gladding, R. L.; Hong, J.; Halldin, C.; Pike, V. W.; Innis, R. B. The PET radioligand [¹¹C]MePPEP binds reversibly and with high specific signal to cannabinoid CB₁ receptors in nonhuman primate brain. *Neuropsychopharmacology* **2008**, *33*, 259–269.

(30) Laruelle, M.; Slifstein, M.; Huang, Y. Relationships between radiotracer properties and image quality in molecular imaging of the

brain with positron emission tomography. *Mol. Imaging Biol.* **2003**, *5*, 363–375.

(31) Waterhouse, R. N. Determination of lipophilicity and its use as a predictor of blood-brain barrier penetration of molecular imaging agents. *Mol. Imaging Biol.* **2003**, *5*, 376–389.

(32) Andersson, Y.; Långström, B. Transition metal-mediated reactions using [¹¹C]cyanide in synthesis of ¹¹C-labeled aromatic-compounds. *J. Chem. Soc., Perkin Trans. 1* **1994**, *11*, 1395–1400.

(33) Ponchant, M.; Hinnen, F.; Demphel, S.; Crouzel, C. [¹¹C]Copper(I) cyanide: a new radioactive precursor for ¹¹C-cyanation and functionalization of haloarenes. *Appl. Radiat. Isot.* **1997**, *48*, 755–762.

(34) Mathews, W. B.; Monn, J. A.; Ravert, H. T.; Holt, D. P.; Schoepp, D. D.; Dannals, R. F. Synthesis of a mGluR₅ antagonist using [¹¹C]copper(I) cyanide. *J. Label. Compd. Radiopharm.* **2006**, *49*, 829–834.

(35) Carson, R. E. PET physiological measurements using constant infusion. *Nucl. Med. Biol.* **2000**, *27*, 657–660.

(36) Jaffe, H.; Leffler, J. E. Synthesis of benziodathiazoles. *J. Org. Chem.* **1975**, *40*, 797–799.

(37) Grosscurt, A. C.; Vanhes, R.; Wellinga, K. 1-Phenylcarbamoyl-2-pyrazolines, a new class of insecticides. 3. Synthesis and insecticidal properties of 3,4-diphenyl-1-phenylcarbamoyl-2-pyrazolines. *J. Agric. Food Chem.* **1979**, *27*, 406–409.

(38) Airaksinen, A. J.; Andersson, J.; Truong, P.; Karlsson, O.; Halldin, C. Radiosynthesis of [¹¹C]ximelagatran via palladium catalyzed [¹¹C]cyanation. *J. Label. Compd. Radiopharm.* **2008**, *51*, 1–5.

(39) Cheng, Y.; Prusoff, W. H. Relationship between the inhibition constant (Kᵢ) and the concentration of inhibitor which causes 50% inhibition (IC₅₀) of an enzymatic reaction. *Biochem. Pharmacol.* **1973**, *22*, 3099–108.

(40) Christman, D. R.; Finn, R. D.; Karlstrom, K. I.; Wolf, A. P. Production of ultra high activity ¹¹C-labeled hydrogen-cyanide, carbon-dioxide, carbon-monoxide, and methane via ¹⁴N(p,α) ¹¹C reaction. *Intl. J. Appl. Radiat. Isot.* **1975**, *26*, 435–442.

(41) Foged, C.; Halldin, C.; Hiltunen, J.; Braestrup, C.; Thomsen, C.; Hansen, H. C.; Suhara, T.; Pauli, S.; Swahn, C. G.; Karlsson, P.; Larsson, S.; Farde, L. Development of ¹²³I-labelled NNC 13-8241 as a radioligand for SPECT visualization of benzodiazepine receptor binding. *Nucl. Med. Biol.* **1996**, *23*, 201–209.

(42) Clark, J. D.; Baldwin, R. L.; Bayne, K. A.; Brown, M. J.; Gebhart, G. F.; Gonder, J. C.; Gwathmey, J. K.; Keeling, M. E.; Kohn, D. F.; Robb, J. W.; Smith, O. A.; Steggerda, J.-A. D.; VandeBer, J. L. *Guide for Care and Use of Laboratory Animals*; National Academies Press: Washington, DC, 1996.

(43) Karlsson, P.; Farde, L.; Halldin, C.; Swahn, C. G.; Sedvall, G.; Foged, C.; Hansen, K. T.; Skrumsager, B. PET examination of [¹¹C]NNC-687 and [¹¹C]NNC-756 as new radioligands for the D₁-dopamine receptor. *Psychopharmacology* **1993**, *113*, 149–156.

(44) Wienhard, K.; Dahlbom, M.; Eriksson, L.; Michel, C.; Bruckbauer, T.; Pietrzyk, U.; Heiss, W. D. The ECAT Exact HR: Performance of a new high-resolution positron scanner. *J. Comput. Assist. Tomogr.* **1994**, *18*, 110–118.

(45) Roland, P. E.; Graufelds, C. J.; Wåhlin, J.; Ingelman, L.; Andersson, M.; Ledberg, A.; Pedersen, J.; Åkerman, S.; Dabringhaus, A.; Zilles, K. Human brain atlas: for high-resolution functional and anatomical mapping. *Human Brain Mapping* **1994**, *1*, 173–184.

(46) Halldin, C.; Swahn, C. G.; Farde, L.; Sedvall, G. Radioligand disposition and metabolism. In *PET for Drug Development and Evaluation*; Comar, D. Ed.; Kluwer Academic Publishers: Dordrecht, Netherlands, 1995; pp 55−65.